Expert Systems with Applications 39 (2012) 1459–1473

Contents lists available at SciVerse ScienceDirect

Expert Systems with Applications

journal homepage: www.elsevier.com/locate/eswa

An advanced scatter search design for skull-face overlay in craniofacial superimposition

Oscar Ibáñez [a,*], Oscar Cordón [a,c], Sergio Damas [a], José Santamaría [b]

[a] European Centre for Soft Computing, Mieres, Spain
[b] Department of Computer Science, University of Jaén, Jaén, Spain
[c] Department of Computer Science and A.I., E.T.S.I. Informática y Telecomunicación, University of Granada, Granada 18071, Spain

ARTICLE INFO

Keywords:
Forensic identification
Craniofacial superimposition
Skull-face overlay
Image registration
Evolutionary algorithms
Scatter search
CMA-ES

ABSTRACT

Craniofacial superimposition is a forensic identification technique where photographs or video shots of a missing person are compared with a skull found in order to determine whether that is the same person. The second stage of this complex forensic process, named skull-face overlay, aims to achieve the best overlay of the skull 3D model and the 2D image of the face. In this paper, we aim to propose a new skull-face overlay method based on the scatter search evolutionary algorithm. This new design exploits problem-specific information in order to achieve faster and more robust solutions. The performance of our proposal is compared to the current best performing approach in the field of automatic skull-face overlay. Results on six real-world identification cases previously solved by the Physical anthropology lab at the University of Granada (Spain) are considered in our experimental study. The proposed method has shown a very accurate and robust performance when solving the latter six face-skull overlay problem instances.

1. Introduction

One of the most outstanding research areas in forensic medicine is human identification. When this task is done from the study of some skeleton remains, we refer to the area of forensic anthropology (Burns, 2007). In the last few decades, anthropologists have focused their attention on improving those techniques that allow a more accurate identification. Hence, forensic identification has become a very active research area nowadays.

Before making a decision on the identification, there is a need to follow different procedures that let the forensic experts assign a sex, age, human group, and height to the subject from the study of the bones found. Once the sample of candidates for identification is constrained by these preliminary studies, a specific identification technique is applied. Among those available in the discipline, *craniofacial superimposition* (Iscan, 1993; Krogman & Iscan, 1986; Stephan, 2009) is a forensic process where photographs or video shots of a missing person are compared with the skull that is found. By projecting both photographs on top of each other (or, even better, matching a scanned three-dimensional skull model against the face photo/series of video shots), the forensic anthropologist can try to establish whether that is the same person.

The craniofacial superimposition process is known to be one of the most time consuming tasks for the forensic experts (it takes up to 24 h in many real world situations). In addition, there is not a systematic methodology but every expert usually applies a particular process. Hence, there is a strong interest in designing automatic methods to support the forensic anthropologist to put it into effect (Ubelaker, 2000).

In our view, when considering an advanced 3D computer-based craniofacial superimposition system, the whole process is composed of the following three stages (Damas et al., in press):

1. The first stage involves achieving a digital model of the skull and enhancing the image of the face. Obtaining of an accurate 3D model of the subject of the identification process, i.e. the human skull, is nowadays an affordable and attainable activity. To do so, a laser range scanner like the one used by our team (Fig. 1), available in the Physical Anthropology Lab at the University of Granada (Spain), and a manual or automatic 3D reconstruction procedure (Santamaría, Cordón, Damas, Alemán, & Botella, 2007; Santamaría, Cordón, Damas, García-Torres, & Quirin, 2009) is considered. Concerning the image of the face, the most recent systems use a 2D digital image and consider the use of typical image processing algorithms (Gonzalez & Woods, 2002) to enhance its quality.
2. The second stage is the skull-face overlay. It consists of searching for the best overlay of the skull 3D model and the 2D image of the face achieved during the first stage. This is usually done by bringing to match some corresponding anthropometrical landmarks on the skull and the face.

* Corresponding author. Tel.: +34 985 456545; fax: +34 985 456699.
E-mail address: oscar.ibanez@softcomputing.es (O. Ibáñez).

0957-4174/$ - see front matter © 2011 Elsevier Ltd. All rights reserved.
doi:10.1016/j.eswa.2011.08.034

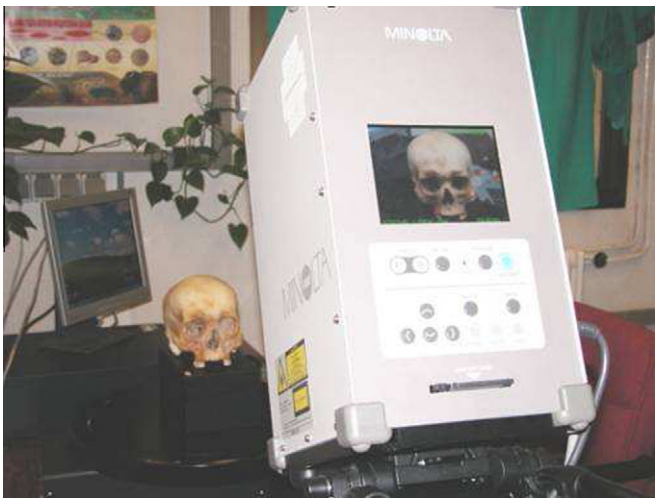

Fig. 1. Acquisition of a skull 3D partial view using a Konica–Minolta™ laser range scanner.

3. Finally, the third stage of the craniofacial superimposition process corresponds to the decision making. Based on the skull-face overlay achieved, the identification decision is made by either judging the matching between the corresponding landmarks in the skull and in the face, or by analyzing the respective profiles.

The current paper focuses on the second stage of the craniofacial superimposition process, the skull-face overlay. More in detail, we try to exploit the benefits of applying *scatter search* (SS) (Laguna & Martí, 2003) to develop this task in an automatic way (under the supervision of the forensic experts). Our intention is to provide a faster and more accurate algorithm than those in the literature. In particular, we aim to ensure a faster approach (in terms of convergence) than our previous proposal (Ibáñez, Ballerini, Cordón, Damas, & Santamaría, 2009), based on the use of CMA-ES (Hansen & Ostermeier, 2001), which is the current best performing approach in the field of automatic skull-face overlay. In fact, CMA-ES is considered as the state-of-the-art evolutionary strategy and it has been widely used in many real world applications (Gagné, Beaulieu, Parizeau, & Thibault, 2008; Kämpf & Robinson, 2009; Tvrdík, 2009).

To do so, our SS design relies on: (i) the use of a population size several times lower than the one typically defined with genetic algorithms; (ii) the generation of an initial population spread throughout the search space, in order to encourage diversification; (iii) the initialization of the population based on the delimitation of the rotation angles using problem-specific information (domain knowledge), in order to reduce the search space, thus decreasing the convergence time and increasing the robustness; (iv) the establishment of a systematic solution combination criterion to favor the search space intensification; and (v) the use of local search to achieve a faster convergence to promising solutions (see Section 3.3.3).

The proposed method has been validated over six different real-world identification cases previously addressed by the staff of the Physical Anthropology lab at the University of Granada in collaboration with the Spanish scientific police, following a computer supported but manual approach for craniofacial superimposition. It provided highly satisfactory results in terms of accuracy and convergence in comparison with the existing CMA-ES-based approach.

The structure of this paper is as follows. In Section 2 we describe the skull-face overlay problem and the methods considered in the literature to solve it. Section 3 describes our proposal, which is tested in Section 4 over six different skull-face overlay problem instances. Finally, in Section 5 we present some conclusions and new open lines for future works.

2. Skull-face overlay in craniofacial superimposition

The success of the overlay technique requires positioning the skull in the same pose of the face as seen in the given photograph (provided by the relatives of the missing/deceased person). The orientation process is a very challenging and time-consuming part of the craniofacial superimposition technique (Fenton, Heard, & Sauer, 2008).

Most of the existing skull-face overlay methods are guided by a number of anthropometrical landmarks located in both the skull and the photograph of the missing person (see Figs. 2 and 3, respectively). The selected landmarks are placed in those parts where the thickness of the soft tissue is low. The goal is to ease their location when the anthropologist must deal with changes in age, weight, and facial expressions.

Once these landmarks are available, the skull-face overlay procedure is based on searching for the skull orientation leading to the best matching of the set of landmarks.

In view of the task to be performed, the relation of the desired procedure with the image registration (IR) problem in computer vision (Zitova & Flusser, 2003) can be clearly identified. In the

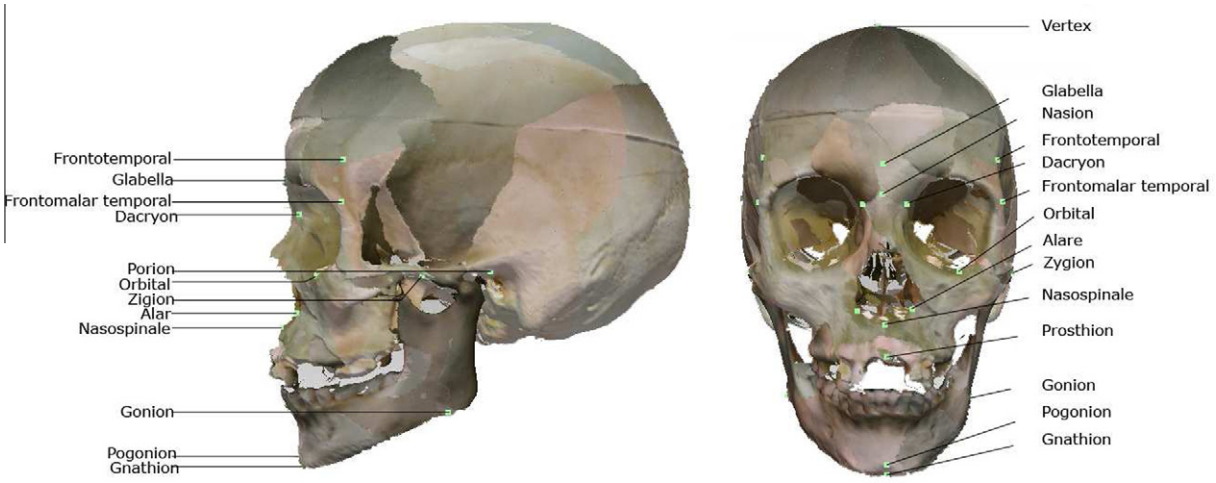

Fig. 2. Principal craniometric landmarks: lateral (left) and frontal (right) views.

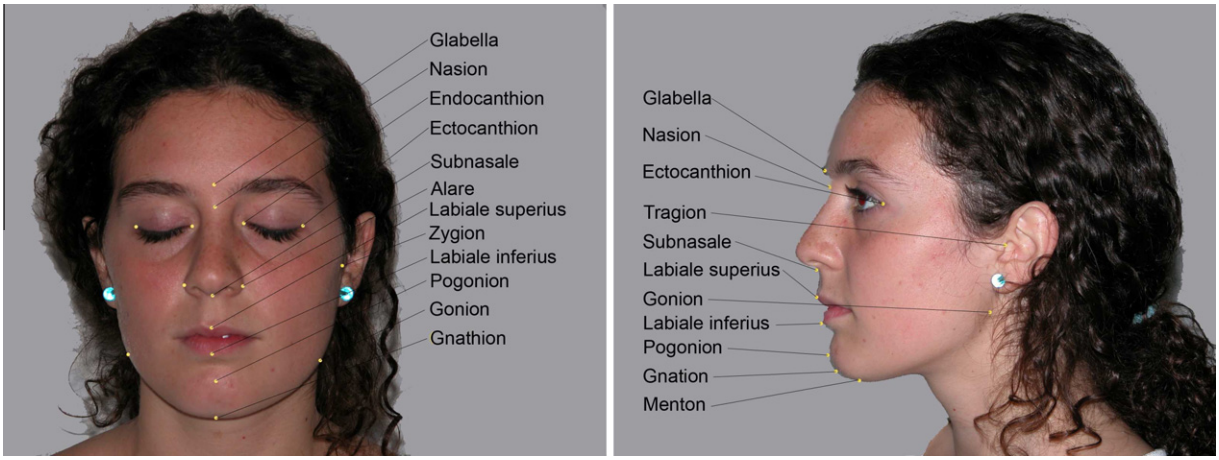

Fig. 3. Principal facial landmarks: lateral (left) and frontal (right) views.

following subsection, we explain the reasons why the skull-face overlay forensic task is modeled as an IR optimization problem, and we summarize the existing approaches to deal with it.

2.1. Skull-face overlay as an image registration problem

IR (Zitova & Flusser, 2003) is a fundamental task in image analysis. It aims to find a correspondence (or transformation) among two or more images taken under different conditions, i.e. at different times, from different viewpoints, using different sensors, or a combination of them. Thus, the key idea of the IR process is achieving the transformation (rotation, translation, etc.) that places different images in a common coordinate system bringing the points as close together as possible. This is done by an optimization process which aims to minimize the error of a given metric of resemblance. Evolutionary algorithms (EAs) (Eiben & Smith, 2003) in general, and genetic algorithms (GAs) (Michalewicz, 1996) in particular, have been successfully applied to tackle different IR problems (Cordón, Damas, & Santamaría, 2006; Cordón, Damas, & Santamaría, 2007; Rouet, Jacq, & Roux, 2000; Silva, Bellon, & Boyer, 2005; Yamany, Ahmed, & Farag, 1999).

In view of the latter, a sensible way to design an automatic skull-face overlay procedure is through the use of a 3D-2D IR technique to properly align the skull 3D model and the 2D image of the face in a common coordinate frame. However, solving the skull-face overlay problem in the latter fashion results in a really complex optimization task, with a highly multimodal landscape, and forensic experts demand highly robust and precise results. This complex landscape leaded us to propose different evolutionary methods (Ibáñez et al., 2009) such as CMA-ES (Hansen & Ostermeier, 2001) and different real-coded GAs (Herrera, Lozano, & Verdegay, 1998), achieving really good results (as we will show in the following section).

2.2. Problem solving methods

Most of the methods tackling the craniofacial superimposition problem focus on the skull-face overlay stage. Some of these approaches were classified in a review by Aulsebrook, Iscan, Slabbert, and Becker (1995) according to the technology they used, i.e. static photographic transparency, video technology, and computer graphics. In a previous paper (Damas et al., in press) we reviewed craniofacial superimposition considering an up-to-date classification criterion, related to the use of computers.

Recent papers confirm that some authors think the most advanced method is based on a manually performed digital superimposition supported by the use of the imaging tools provided by the Adobe Photoshop® and Corel Draw® software packages (Al-Amad, McCullough, Graham, Clement, & Hill, 2006; Bilge, Kedici, Alakoc, Ulkuer, & Ilkyaz, 2003; Ross, 2004). It is worth mentioning that the forensic expert may even employ up to 24 h for each case, working in the latter way.

Up to our knowledge, there are only three proposals performing skull-face overlay in a fully automatic way, based on the use of neural networks (Ghosh & Sinha, 2001), binary-coded GAs (Nickerson, Fitzhorn, Koch, & Charney, 1991), and real-coding EAs (Ibáñez et al., 2009), respectively. However, as we will see in the following, the former two are not suitable for forensic experts.

The method proposed by Ghosh and Sinha Ghosh and Sinha (2001) was an adaptation of their previous proposal for face recognition problems (Sinha, 1998). The extended symmetry perceiving adaptive neuronet (ESPAN) consisted of two neural networks to be applied to two different parts of the overlaying. It allows the user to select fuzzy facial features to account for ambiguities due to soft tissue thickness. More in details, the system was able to implement an objective assessment of the symmetry between two nearly front images, the cranial image and the facial image, which were the inputs and played the role of the source and the target images, respectively. The output was the mapped cranial image suitable for superimposition. Two networks needed to be trained separately because each of them was able to correctly map only a part of the cranial image. Two limitations, already pointed out by the authors, were the existence of a part of the cranial image that would never be properly mapped and the need of a frontal view image. In addition, the method is only valid for 2D images, i.e., it is not able to handle a 3D skull model but just a less informative 2D skull photograph. Finally it was not fully applicable because of its long computation time and the need of separately applying two different networks to the upper skull contour and to frontal view cranial features. The skull-face overlay found by the first one could be disrupted by the second.

Nickerson et al.'s method (Nickerson et al., 1991) used a binary-coded GA (BCGA) to find the optimal parameters of the similarity and perspective transformation that overlays the 3D skull model on the face photograph. More in details, this method included the following tasks:

- 2D digitalization of an antemortem facial photograph.
- 3D digitalization of the surface mesh of the skull.
- Application of digital filtering techniques to the 2D photo image and the 3D model to reduce or eliminate systematic error.
- Selection of four landmark points on the digital facial image and four equivalent non-coplanar landmarks on the skull surface mesh.

- Calculation of the near-optimal affine and perspective transformations required to map the skull surface mesh into two dimensions and onto the image of the face.
- Joint solid rendering of the digital facial photograph and transformed skull surface mesh for visual analysis.

A digital camera and a laser range scanner were used for 2D and 3D digitalizations, respectively. Well known image processing algorithms were considered for image enhancement. Rendering was done through computer graphics techniques, after polygonal texture mapping of the 2D image. The automatic calculation of the mapping of the skull surface mesh on the digital facial photograph was achieved from the matching of the four landmarks previously identified both in the face and the skull.

Finally, in Ibáñez et al. (2009) we proposed a new formulation (see Section 3.1 for more details) for the skull-face overlay task, considering it as a numerical optimization problem with twelve unknowns representing the geometric transformation underlying the corresponding 3D-2D IR process. We also proposed and tested four new evolutionary methods (including an adaption of Nickerson et al.'s proposal) to solve this optimization problem based on the use of a BCGA, two real-coded GAs, and the CMA-ES. The best results, achieved using CMA-ES, were really competitive in terms of performance and robustness with the human-obtained superimpositions. In contrast, Nickerson et al.'s method was not able to achieve suitable results over none of the six real-world cases of study presented in the paper.

3. A scatter search method for skull-face overlay

Our proposal tries to solve a 3D-2D skull-face overlay task as a numerical optimization problem. The goal is to find a near-optimal geometric transformation, competitive enough considering convergency and accuracy criteria when comparing to the state-of-the-art method, CMA-ES, which has shown to be competitive with the forensic expert manual overlays (Ibáñez et al., 2009). To do so, we will use an efficient stochastic optimization technique named scatter search (Laguna & Martí, 2003), guided by the matching of the two different sets of corresponding landmarks described in Section 2.

The following subsections are denoted to respectively introduce the problem formulation considered (taken from our previous work Ibáñez et al., 2009), the basics of SS, and the specific design considered for each of the SS components to solve our problem.

3.1. Problem formulation

Given two sets of 2D facial and 3D cranial landmarks (F and C, respectively):

$$F = \begin{bmatrix} x_{f_1} & y_{f_1} & 1 & 1 \\ x_{f_2} & y_{f_2} & 1 & 1 \\ \vdots & \vdots & \vdots & \vdots \\ x_{f_N} & y_{f_N} & 1 & 1 \end{bmatrix} C = \begin{bmatrix} x_{c_1} & y_{c_1} & z_{c_1} & 1 \\ x_{c_2} & y_{c_2} & z_{c_2} & 1 \\ \vdots & \vdots & \vdots & \vdots \\ x_{c_N} & y_{c_N} & z_{c_N} & 1 \end{bmatrix}$$

we aim to solve the following system of equations with twelve unknowns $(r_x, r_y, r_z, d_x, d_y, d_z, \theta, s, t_x, t_y, t_z, \phi)$ that represents the geometric transformation which maps every cranial landmark C_i in the skull 3D model onto its corresponding facial landmark F_i in the photograph:

$$F = C \cdot (A \cdot D_1 \cdot D_2 \cdot \theta \cdot D_2^{-1} \cdot D_1^{-1} \cdot A^{-1}) \cdot S \cdot T \cdot P \quad (1)$$

A brief description of the set of geometric transformations needed to accomplish the overlay task follows (a more detailed description is to be found in Ibáñez et al. (2009)). We should notice that a detailed explanation of projective geometry is out of the scope of this contribution, the interested reader is referred to Foley (1995).

- **Rotation** R. The first step to find the proper location of the skull will involve applying a rotation to orient the skull in the same pose of the photograph. In order to define a rotation, the direction of the rotation axis $\vec{d} = (d_x, d_y, d_z)$, the location of the rotation axis with respect to the center of coordinates $\vec{r} = (r_x, r_y, r_z)$, and the angle θ must be given. This rotation process R is thus given by:

$$R = \left(A \cdot D_1 \cdot D_2 \cdot \Theta \cdot D_2^{-1} \cdot D_1^{-1} \cdot A^{-1}\right) \quad (2)$$

where:

$$A = \begin{bmatrix} 1 & 0 & 0 & 0 \\ 0 & 1 & 0 & 0 \\ 0 & 0 & 1 & 0 \\ -r_x & -r_y & -r_z & 1 \end{bmatrix} \quad D_1 = \begin{bmatrix} 1 & 0 & 0 & 0 \\ 0 & d_z/v & d_y/v & 0 \\ 0 & -d_y/v & d_z/v & 0 \\ 0 & 0 & 0 & 1 \end{bmatrix}$$

$$D_2 = \begin{bmatrix} v & 0 & d_x & 0 \\ 0 & 1 & 0 & 0 \\ -d_x & 0 & v & 0 \\ 0 & 0 & 0 & 1 \end{bmatrix}$$

$$\Theta = \begin{bmatrix} \cos\Theta & -\sin\Theta & 0 & 0 \\ \sin\Theta & \cos\Theta & 0 & 0 \\ 0 & 0 & 1 & 0 \\ 0 & 0 & 0 & 1 \end{bmatrix} \quad v = \sqrt{d_y^2 + d_z^2}$$

- **Scaling** S. The size of the skull model must be uniformly adapted according to the size of the missing person in the photograph. Hence, the coordinates of each point of the skull model will be resized considering a factor named s:

$$S = \begin{bmatrix} s & 0 & 0 & 0 \\ 0 & s & 0 & 0 \\ 0 & 0 & s & 0 \\ 0 & 0 & 0 & 1 \end{bmatrix}$$

- **Translation** T. The coordinates of the skull model are relative to the origin defined by the range scanner. Thus, it must be translated according to $T = (t_x, t_y, t_z)$ in order to be located in front of the camera and reproduce the conditions when the photograph of the missing person was taken. To do so, the following matrix is considered:

$$T = \begin{bmatrix} 1 & 0 & 0 & 0 \\ 0 & 1 & 0 & 0 \\ 0 & 0 & 1 & 0 \\ t_x & t_y & t_z & 1 \end{bmatrix}$$

- **Perspective projection** P. In computer graphics, cameras perspective projection is modeled defining a frustum[1] of a rectangular pyramid (Fig. 4, left). There are thus two planes, near clipping plane (NCP) and far clipping plane (FCP), which are used to delimit what is visible in the scene and what is consequently represented in the computer (those parts between both planes). In our case, once the previous transformations are applied, we need to determine how far the camera is from the skull. This issue has a strong connection to the angle of view (ϕ) of the camera, which describes the angular extent of a given scene that is imaged by a camera. Fig. 4 depicts this effect. Once the camera

[1] A frustum is the portion of a solid –normally a cone or a pyramid– which lies between two parallel planes cutting the solid.

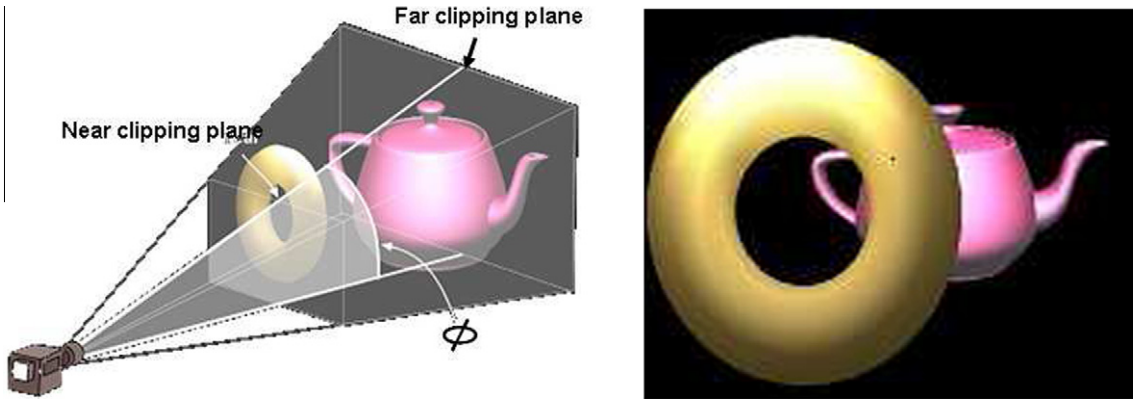

Fig. 4. Camera configuration with angle of view ϕ (left) and the corresponding photograph (right).

is located in the proper position, all the rays connecting every 3D landmark of the skull with its corresponding 2D landmark in the photograph will converge in the center of projection.
The perspective transformation described is thus given by:

$$P = \begin{bmatrix} 1 & 0 & 0 & 0 \\ 0 & 1 & 0 & 0 \\ 0 & 0 & \tan(\phi/2) & \tan(\phi/2) \\ 0 & 0 & 0 & 1 \end{bmatrix}$$

3.2. Basis of scatter search

SS fundamentals were originally proposed by Fred Glover in Glover (1977) and have been later developed in some texts like (Laguna & Martí, 2003). The main idea of this technique is based on a *systematic* combination between solutions (instead of a randomized one like that usually done in GAs) taken from a considerably reduced evolved pool of solutions named Reference set (between five and ten times lower than usual GA population sizes) as well as on the typical use of a local optimizer. This way, an efficient and accurate search process is encouraged thanks to the latter and to other innovative components we will describe later. The general SS approach is graphically shown in Fig. 5:

3.3. Scatter search-based skull-face overlay method implementation

The fact that the mechanisms within SS are not restricted to a single uniform design allows the exploration of strategic possibilities that may prove effective in a particular implementation. Of the five methods in the SS methodology, only four are strictly required. The improvement method is usually needed if high quality

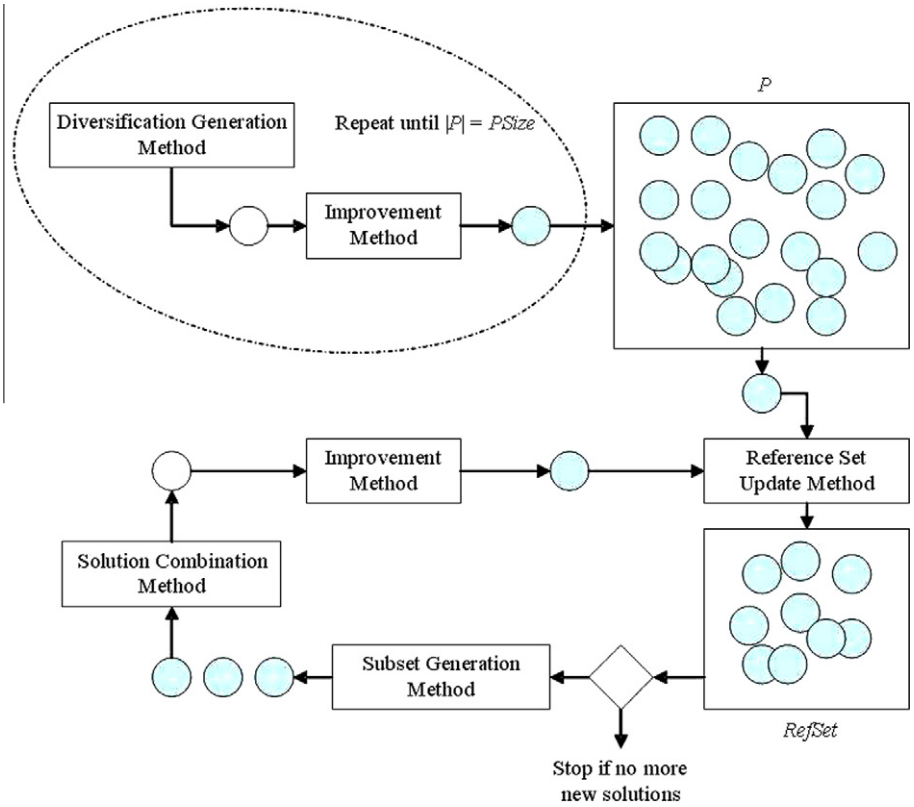

Fig. 5. The control diagram of SS.

$P \leftarrow \emptyset$

While ($|P| < PSize$) do

Obtain a new solution x generated by the **Diversification Generation Method**

Improve x with the **Improvement Method** generating a solution x'

If $x' \notin P$ Then $P \leftarrow P \cup \{x'\}$

Sort the solutions in P according to their objective function value (the best overall solution in P, that one with the lowest F value, is the first in such list). Add the first b solutions from P to $RefSet$

While (not reached the stop stopping condition) do

$NewElements \leftarrow$ True

$Pool \leftarrow \emptyset$

While ($NewElements$) and (not reached the stopping condition) do

Generate all the subsets of (pairs of) solutions $s_i = \{x_j, x_k\}$ ($\{x_j, x_k\} \in Subsets \mid x_j, x_k \in Refset \wedge j, k = \{1, \cdots, \mid RefSet \mid\} \wedge j \neq k$) with the **Subset Generation Method**

$NewElements \leftarrow$ False

While ($Subsets \neq \emptyset$) do

Select the next subset s_i ($i = \{1, \cdots, \frac{b\cdot(b-1)}{2}\}$)from $Subsets$ and delete it from $Subsets$

Apply the **Solution Combination Method** to the next pair of solutions $\{x_j, x_k\} \in s_i$ that were not previously combined in order to obtain a new solution x

If ($F(x) < F(x_j)$ OR $F(x) < F(x_k)$) Then

Apply the **Improvement Method** to the solution x to obtain the solution x'

Else $x' \leftarrow x$

Add x' to $Pool$

Apply the **Reference Set Update Method** selecting the best b solutions in $RefSet \cup Pool$

If ($RefSet$ has at least one new solution) Then $NewElements \leftarrow$ True

If (not reached the stop criterion) Then

Build a new set P using the **Diversification Generation Method**

Replace the worst $b - 1$ solutions from $RefSet$ with the best $b - 1$ solutions from P

Fig. 6. Pseudocode of the SS-based skull-face overlay optimizer.

outcomes are desired but a SS procedure can be implemented without it. In the following subsections, we will briefly describe the specific design of each component of our SS-based skull-face overlay method outlined in Fig. 6, where *P* denotes the initial set of solutions generated with the *diversification generation method* (with *Psize* being the size of *P*), the reference set is noted as *RefSet* (with *b* being its size, usually significantly lower than *Psize*), and *Pool* is the set of trial solutions constructed with the *Combination* and *improvement methods* each iteration.

3.3.1. Coding scheme and objective function

As seen, skull-face overlay can be formulated as a numerical optimization problem with twelve unknowns in the framework of IR. In Section 3.1 we described the geometric transformation *f* for the 3D-2D IR problem underlying this forensic task. This transformation *f* is determined fixing the said twelve unknowns. We consider a coding scheme representing them in a vector of real numbers to be evolved by means of the SS algorithm.

To measure the quality of the registration transformation encoded in a specific individual an objective function is needed. Therefore, given $C = \{C_1, C_2, \ldots, C_N\}$ and $F = \{F_1, F_2, \ldots, F_N\}$, two sets of 3D cranial and 2D facial landmarks respectively, we propose the minimization of the following function:

$$ME = \frac{\sum_{i=1}^{N} \| f(C_i) - F_i \|}{N} \tag{3}$$

with $\| \cdot \|$ being the 2D Euclidean distance, N being the number of considered landmarks, F_i being the positions of the 2D landmarks, and $f(C_i)$ being the positions of the transformed 3D landmarks once they have been spatially relocated and projected in the projection plane.

3.3.2. Diversification generation method and advanced heuristic initialization strategy

This method makes use of a controlled randomization based on frequency memory to generate an initial set *P* of *Psize* diverse solutions (Glover, Laguna, & Martí, 2003). We carry out this by dividing the range of each variable (in our case, each one of the twelve geometric transformation parameters) into four sub-ranges of equal size. A solution will be constructed in two steps. First, a sub-range is randomly selected for each variable, where the probability of choosing a sub-range is inversely proportional to its frequency count. Initially, the frequency count for each variable subrange is set to one and the number of times a sub-range *j* has been chosen to generate a value for variable *i* in a solution is accumulated in *frequency_count*(*i*,*j*). Then, as second step, a value is randomly generated within the selected sub-range. Finally, the *improvement method* is applied on the *Psize* solutions generated and the best *b* of them compose the initial *RefSet*.

Using specific information derived from the characteristics of the problem has demonstrated to be an important aid tackling IR problems (Cordón, Damas, Martí, & Santamaría, 2008). In skull-face overlay most of the photographs show a near-forntal pose of the missing person. We found profile pictures in just few cases. We know that we will never tackle a photograph where the missing person is looking backwards. Hence, we propose an initialization of the population based on the delimitation of the rotation angles using the information from the domain knowledge. In order to specify reduced values for the feasible ranges where the twelve parameters will take values, we first orient the skull 3D model towards the camera axis.[2] It is evident that we are only interested in those transformations providing a near front view of the skull, i.e. $\theta \in [-90°, 90°]$ (see Fig. 7) . The advantages of this approach are

[2] Notice that, we can not assume that the initial pose of the skull 3D model is frontal. It may vary depending on the 3D digitalization process.

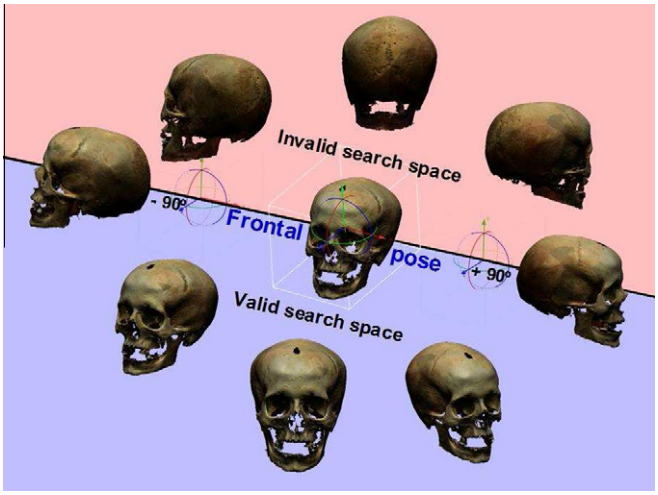

Fig. 7. Search space constrained considering specific information of the problem.

twofold. On the one hand, we will only generate good quality solutions for the initial population. On the other hand, the search space dimension is reduced from 360° to 180°, thus decreasing the convergence time.

To do so, we calculate the centroid, Z, of four non-coplanar cranial landmarks, C_j ($j \in 1,\ldots,4$), in order to estimate the current skull orientation and to rotate properly the skull towards a front view. We also use the maximum distance, r, from Z to the farthest of the said four landmarks ($r = \|Z - C_j\|, j = \{1,\ldots,4\}$) for the proper estimation of the valid ranges of values of the twelve parameters, as follows:

$$r_i \in [Z_i - r,\ Z_i + r], \quad i \in \{x,y,z\}$$
$$d_x, d_y \in [-1,\ 1]$$
$$d_z \in [0,\ 1]$$
$$\theta \in [-90^\circ,\ 90^\circ]$$
$$s \in [0.25,\ 2]$$
$$\phi \in [10^\circ,\ 150^\circ]$$
$$t_x \in [-length_{FB} - (Z_x + r),\ length_{FB} - (Z_x - r)]$$
$$t_y \in [-length_{FB} - (Z_y + r),\ length_{FB} - (Z_y - r)]$$
$$t_z \in [NCP - (Z_z + r),\ FCP - (Z_z - r)]$$

where *FCP* and *NCP* are the far and near clipping planes, respectively; *lengthFB* is the length of the frustum base; and

$$length_{FB} = 1 + FCP * tan\left(\frac{\phi_{max}}{2}\right)$$

In Section 4 we will experimentally demonstrate the benefits of applying this initialization procedure in terms of convergence speed and robustness.

3.3.3. Improvement method

The improvement method is based on XLS, which is a crossover-based local search (LS) method that induces an LS on the neighborhood of the parents solutions involved in crossover (Lozano, Herrera, Krasnogor, & Molina, 2004; Noman et al., 1983). Given a solution to be improved, called family father, L solutions are randomly selected in the current population for mating with the previous one to generate new trial solutions in the father's neighborhood by performing crossover operations. Finally, a selection operation is carried out for replacing the family father with the best solution of the L new solutions only if this one is better than the former. Hence, it can be called *best point neighborhood strategy* (Noman et al., 1983). This procedure is repeated until the considered stop criterion is reached.

In this work, we considered the PBX-α crossover operator (Lozano et al., 2004) (with $\alpha = 0.5$) to generate four neighboring solutions every LS iteration.

3.3.4. Subset generation method

This method generates a collection of solution subsets (noted as *Subsets* in Fig. 6) of the reference set as a basis for creating new combined solutions. In our implementation, the subsets are composed of all the possible pairs of solutions in *RefSet*, so $\frac{b\cdot(b-1)}{2}$ different subsets are generated at each iteration.

3.3.5. Solution combination method

It is based on the use of the BLX-α crossover operator (Eshelman, 1993), commonly used in real-coded GAs. This combination mechanism obtains a trial solution, $x = (h_1,\ldots,h_k,\ldots,h_l)$ (with $l = 12$ being the number of parameters of the geometric transformation and h_k being a given value for such kth variable) from the two parent solutions $x^1 = (c_1^1,\ldots,c_l^1)$ and $x^2 = (c_1^2,\ldots,c_l^2)$ composing a given subset s (see Fig. 6). The offsprings is obtained by uniformly generating a random value for each variable h_k in the interval $[c_{min} - I\cdot\alpha, c_{max} + I\cdot\alpha]$, with $c_{max} = \max(c_k^1, c_k^2), c_{min} = \min(c_k^1, c_k^2)$, and $I = c_{max} - c_{min}$. Hence, the parameter α allows us to make this crossover as disruptive as desired. Such combination method was successfully incorporated to SS in Santamaría et al. (2007), Santamaría et al. (2009), Herrera, Lozano, and Molina (2006).

In our real-world application, we think that applying the improvement method to every trial solution could excessively decrease the exploratory capabilities of the global search strategies of the SS. Indeed, as stated in Krasnogor and Smith (2005), "The majority of memetic algorithms in the literature (in this case, SS) apply local search to every individual in every generation of the evolutionary algorithm, our model makes it clear that this is not mandatory". Hence, we have considered a particular selective application criteria for the improvement method. It is easy to implement and we have recently obtained promising results tackling the IR problem using it in Santamaría et al. (2009). This criterion considers a deterministic scheme, in which the trial solution will be improved using the Improvement Method only if it is better than any of its parents. It has been demonstrated that this strategy is more suitable than others based on random schemes (Santamaría et al., 2009).

3.3.6. Reference set update method

A static strategy for updating the *RefSet* is carried out: first, the Pool set is built by solution combination of all the pairs of solutions being considered and next, the RefSet is updated with the solutions of the Pool set according to quality criterion.

4. Experiments

This section is devoted to develop an experimental study allowing us to validate the performance of the new SS-based skull-face overlay process proposed in this contribution. To do so, we first introduce the six different real-world skull-face overlay problems to be tackled, and then we show the parameter setting considered in the experiments. Next, we present the obtained results and their analysis. A comparison with respect to CMA-ES, the state-of-the-art method to solve the skull-face overlay forensic task, is carried out.

4.1. Cases of study and experimental setup

Our experimental study will involve six different skull-face overlay problem instances, corresponding to four real-world cases previously addressed by the staff of the Physical Anthropology lab

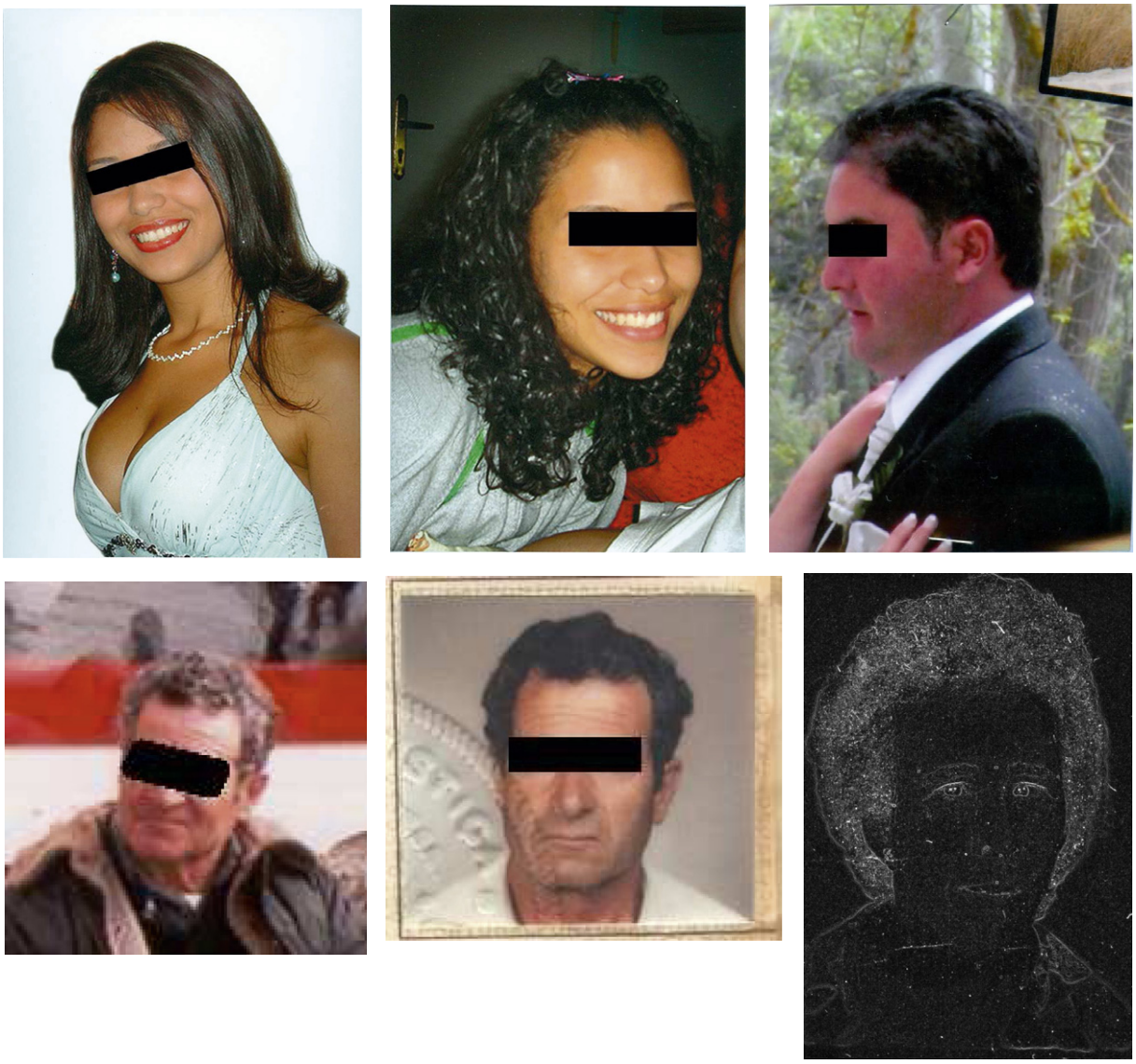

Fig. 8. Face photographs of the missing people. The three images in the first row correspond to the case study 1-poses 1 and 2, and case study 2 (a single photograph). In the second row, from left to right, poses 1 and 2 of case study 3, and case study 4 (a single photograph).

at the University of Granada in collaboration with the Spanish scientific police. Those four identification cases were solved following a computer-supported but manual approach for craniofacial superimposition (see Section 2.2). We will consider the 2D photographs of the missing people (Fig. 8) and their corresponding 3D skull models (Fig. 9) acquired at the lab by using its Konica–Minolta© 3D Lasserscanner VI-910.

The first case of study happened in Cádiz, Spain. The two first photographs shown in the first row of Fig. 8 belong to this first case of study. They were provided by the family, that acquired them at different moments and in different poses and conditions. Hence this case consists of two distinct skull-face overlay problem instances.

The forensic anthropologists manually selected a large set of 3D landmarks on the skull. On the other hand, the 2D landmarks selected on the face photographs were eight and twelve for poses 1 and 2, respectively. Indeed, not all the landmarks are visible in all the poses. Of course, only the corresponding 3D-2D landmarks are used for solving the two superimposition instances.

The second case of study is related with the skeleton remains of an old man found in the surroundings of Granada, Spain. Only one photograph, in a completely lateral pose was provided by the family. The forensic experts identified seven 2D landmarks on it.

The third case of study happened in Granada, Spain. The two photographs shown in the left-hand side of the second row of Fig. 8, acquired at different moments, were provided by the family. Hence, this case consists of two different skull-face overlay instances for which, the forensic anthropologists manually selected eight and fourteen 2D landmarks in the first and second photograph, respectively.

The last case of study corresponds to a missing lady found in Mallorca, Spain. Only one photograph[3] (the last one in the second row of Fig. 8) where our forensic experts were able to locate six 2D landmarks, was provided by the family.

Regarding the experimental setup we will first study the performance of the proposed SS algorithm considering different settings. For that aim, we will start by analyzing its behavior when considering and not considering the advanced initialization approach proposed in Section 3.3.2, i.e., applying and not applying the

[3] Notice that, it has been processed due to legal reasons.

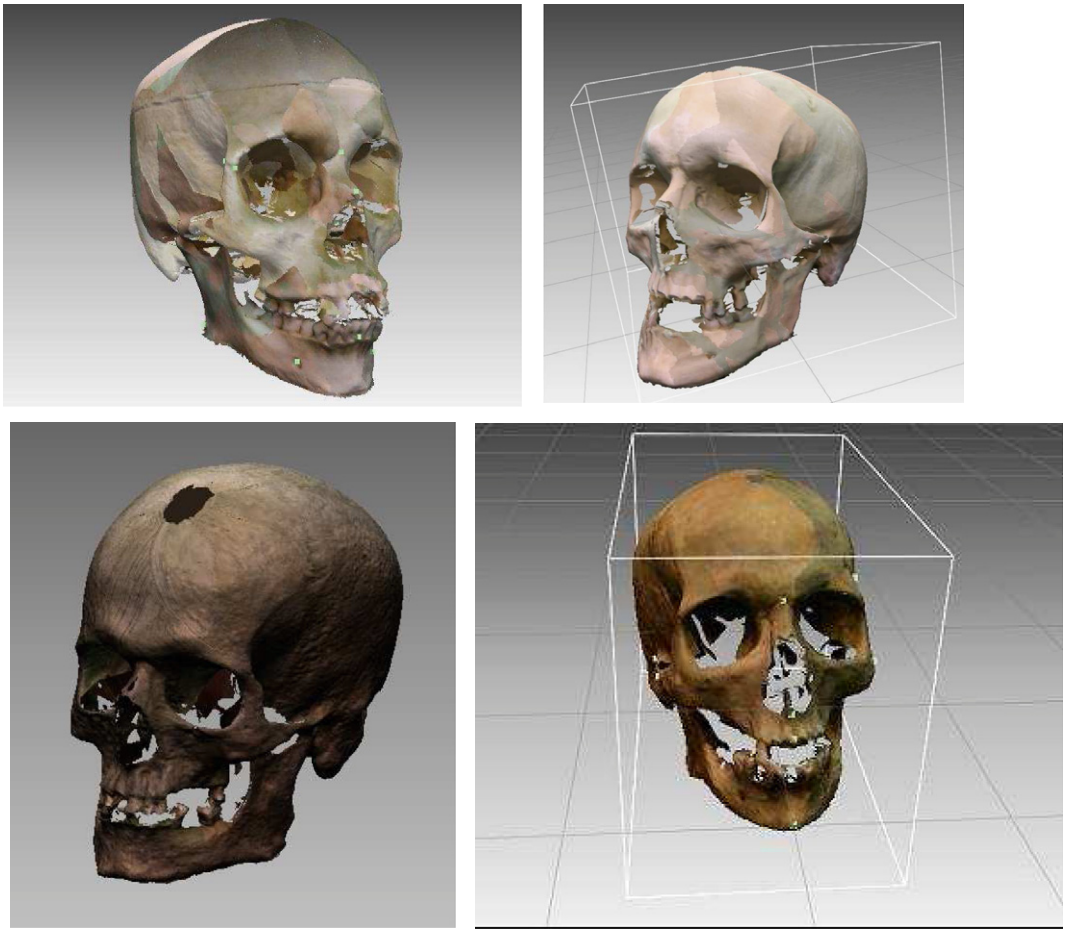

Fig. 9. From left to right. 3D skull model of cases of study 1, 2, 3, and 4.

restriction of the rotation angles. Then, we will compare its performance with that of CMA-ES in terms of accuracy, robustness, and convergence speed. Different experiments were done considering several values for the number of evaluations (30000, 60000, 100000, 150000, and 300000) in order to compare convergence speed.

For the SS, the initial diverse set P comprises $Psize = 30$ solutions and the *RefSet* is composed of the $b = 12$ best ones of them. BLX-α is applied with $\alpha = 1$ (Lozano, Herrera, Krasnogor, & Molina, 2004), while the *improvement method* is selectively applied during 40 iterations each time.

In the case of CMA-ES, the following values are taken for the different parameters:

Initial θ (mutation distribution variance) = 0.1
λ (population size, offspring number) = 100
μ (number of parents/points for recombination) = 15

In addition, the restart operator (Auger et al., 2005), which does not increase the population size, is used every 25000 evaluations to avoid the convergence of the algorithm to local minima. The rest of the parameters are the default ones, reported in Hansen et al. (1996).

In order to avoid execution dependence, thirty different runs for each parameter setting have been performed and different statistics (best result, worst result, mean, and standard deviation over the thirty runs) are provided. All the methods are run on a PC with an AMD Athlon 64 X2 Dual (2 core 2.59 GHz), 2 GB of RAM and Linux CentOS. We considered the ME (see Eq. (3)) for the assessment of the final superimposition results. Besides, some graphical representations of the obtained overlays are also shown in order to allow for a visual assessment.

4.2. Scatter search-based method results analysis

As it has been mentioned before, we will study the performance of the proposed SS algorithm by comparing its behavior applying and not applying the restriction of the rotation angles, i.e., considering and not considering the advanced initialization strategy, respectively. Tables 1–6 show the corresponding results for each of the six different skull-face overlay cases (belonging to four different real-world cases of study). For each algorithm (SS and CMA-ES), the best (Min.), the worst (Max.), the mean (Mean), and the standard deviation (St.Dev.) values for the fitness function (see Eq. (3)) after thirty runs are showed. The best minimum and mean results in each table are highlighted in boldface.

In view of the results shown in the two top blocks of the tables, we can observe how, in most of the cases, the best minimum result obtained by the algorithm is the same regardless if the initialization strategy is considered or not. Only in one of the problem instances, the first pose of case study 1, the minimum value finally achieved by considering the initialization strategy is better than that obtained without using it (0.015 vs. 0.018, see Table 1). Besides, the derivation of this result requires only developing 30000 evaluations in comparison with the 100000 evaluations performed by the latter SS variant (i.e., the SS variant including the "intelligent" initialization is more than three times faster). In the remaining five instances, the use of the advanced initialization

Table 1
Case study 1, pose 1. Comparison between CMA-ES and SS results. Best minimum and mean values are highlighted in bold letters.

Case	Algorithm	Initialization	Evals (thousands)	Min.	Max.	Mean	St.Dev.
1, Pose 1	SS	No	30	0.021	0.133	0.095	0.036
1, Pose 1	SS	No	60	0.019	0.123	0.052	0.031
1, Pose 1	SS	No	100	0.018	0.097	0.033	0.013
1, Pose 1	SS	No	150	0.018	0.037	0.030	0.005
1, Pose 1	SS	No	300	0.018	0.037	0.028	0.006
1, Pose 1	SS	Yes	30	**0.015**	0.126	0.063	0.041
1, Pose 1	SS	Yes	60	0.015	0.110	0.037	0.023
1, Pose 1	SS	Yes	100	0.015	0.043	0.027	0.011
1, Pose 1	SS	Yes	150	0.015	0.043	0.027	0.011
1, Pose 1	SS	Yes	300	0.015	0.043	0.024	0.010
1, Pose 1	CMA-ES	No	30	**0.015**	0.121	0.069	0.035
1, Pose 1	CMA-ES	No	60	0.015	0.120	0.067	0.032
1, Pose 1	CMA-ES	No	100	0.015	0.057	0.027	0.012
1, Pose 1	CMA-ES	No	150	0.015	0.040	0.023	0.009
1, Pose 1	CMA-ES	No	300	0.015	0.036	**0.020**	0.007
1, Pose 1	CMA-ES	Yes	30	0.035	0.114	0.069	0.025
1, Pose 1	CMA-ES	Yes	60	0.035	0.114	0.069	0.023
1, Pose 1	CMA-ES	Yes	100	0.035	0.098	0.049	0.016
1, Pose 1	CMA-ES	Yes	150	0.035	0.082	0.046	0.014
1, Pose 1	CMA-ES	Yes	300	0.035	0.044	0.038	0.002

Table 2
Case study 1, pose 2. Comparison between CMA-ES and SS results. Best minimum and mean values are highlighted in bold letters.

Case	Algorithm	Initialization	Evals (thousands)	Min.	Max.	Mean	St.Dev.
1, Pose 2	SS	No	30	**0.022**	0.157	0.032	0.024
1, Pose 2	SS	No	60	0.022	0.038	0.024	0.003
1, Pose 2	SS	No	100	0.022	0.027	0.023	0.001
1, Pose 2	SS	No	150	0.022	0.027	0.023	0.001
1, Pose 2	SS	No	300	0.022	0.027	0.023	0.001
1, Pose 2	SS	Yes	30	**0.022**	0.060	0.025	0.008
1, Pose 2	SS	Yes	60	0.022	0.033	**0.022**	0.002
1, Pose 2	SS	Yes	100	0.022	0.024	0.022	0.000
1, Pose 2	SS	Yes	150	0.022	0.023	0.022	0.000
1, Pose 2	SS	Yes	300	0.022	0.023	0.022	0.000
1, Pose 2	CMA-ES	No	30	**0.022**	0.171	0.071	0.060
1, Pose 2	CMA-ES	No	60	0.022	0.171	0.069	0.058
1, Pose 2	CMA-ES	No	100	0.022	0.039	0.024	0.004
1, Pose 2	CMA-ES	No	150	0.022	0.053	0.024	0.006
1, Pose 2	CMA-ES	No	300	0.022	0.046	**0.022**	0.004
1, Pose 2	CMA-ES	Yes	30	0.064	0.165	0.104	0.038
1, Pose 2	CMA-ES	Yes	60	0.063	0.161	0.089	0.031
1, Pose 2	CMA-ES	Yes	100	0.063	0.143	0.070	0.018
1, Pose 2	CMA-ES	Yes	150	0.063	0.098	0.065	0.006
1, Pose 2	CMA-ES	Yes	300	0.063	0.064	0.063	0.000

Table 3
Case study 2. Comparison between CMA-ES and SS results. Best minimum and mean values are highlighted in bold letters.

Case	Algorithm	Initialization	Evals (thousands)	Min.	Max.	Mean	St.Dev.
2	SS	No	30	**0.018**	0.167	0.033	0.026
2	SS	No	60	0.018	0.056	0.028	0.008
2	SS	No	100	0.018	0.054	0.028	0.007
2	SS	No	150	0.018	0.049	0.027	0.007
2	SS	No	300	0.018	0.043	0.026	0.006
2	SS	Yes	30	**0.018**	0.170	0.030	0.026
2	SS	Yes	60	0.018	0.034	0.024	0.004
2	SS	Yes	100	0.018	0.034	0.024	0.004
2	SS	Yes	150	0.018	0.034	0.023	0.004
2	SS	Yes	300	0.018	0.034	0.023	0.004
2	CMA-ES	No	30	**0.018**	0.198	0.110	0.070
2	CMA-ES	No	60	0.018	0.218	0.121	0.065
2	CMA-ES	No	100	0.018	0.083	0.026	0.014
2	CMA-ES	No	150	0.018	0.027	0.023	0.004
2	CMA-ES	No	300	0.018	0.027	**0.020**	0.004
2	CMA-ES	Yes	30	0.103	0.193	0.168	0.022
2	CMA-ES	Yes	60	0.090	0.186	0.145	0.021
2	CMA-ES	Yes	100	0.072	0.178	0.123	0.030
2	CMA-ES	Yes	150	0.070	0.162	0.109	0.022
2	CMA-ES	Yes	300	0.068	0.125	0.088	0.017

Table 4
Case study 3, pose 1. Comparison between CMA-ES and SS results. Best minimum and mean values are highlighted in bold letters.

Case	Algorithm	Initialization	Evals (thousands)	Min.	Max.	Mean	St.Dev.
3, Pose 1	SS	No	30	**0.042**	0.057	0.046	0.004
3, Pose 1	SS	No	60	0.042	0.057	0.046	0.004
3, Pose 1	SS	No	100	0.042	0.057	0.046	0.004
3, Pose 1	SS	No	150	0.042	0.057	**0.045**	0.004
3, Pose 1	SS	No	300	0.042	0.057	0.045	0.004
3, Pose 1	SS	Yes	30	**0.042**	0.061	0.046	0.003
3, Pose 1	SS	Yes	60	0.042	0.060	0.046	0.003
3, Pose 1	SS	Yes	100	0.042	0.060	**0.045**	0.003
3, Pose 1	SS	Yes	150	0.042	0.060	0.045	0.003
3, Pose 1	SS	Yes	300	0.042	0.060	0.045	0.003
3, Pose 1	CMA-ES	No	30	**0.042**	0.284	0.186	0.107
3, Pose 1	CMA-ES	No	60	0.042	0.285	0.189	0.111
3, Pose 1	CMA-ES	No	100	0.042	0.239	0.078	0.066
3, Pose 1	CMA-ES	No	150	0.042	0.218	0.068	0.050
3, Pose 1	CMA-ES	No	300	0.042	0.256	0.053	0.040
3, Pose 1	CMA-ES	Yes	30	0.076	0.284	0.184	0.090
3, Pose 1	CMA-ES	Yes	60	0.076	0.286	0.190	0.089
3, Pose 1	CMA-ES	Yes	100	0.066	0.273	0.094	0.042
3, Pose 1	CMA-ES	Yes	150	0.059	0.186	0.081	0.021
3, Pose 1	CMA-ES	Yes	300	0.060	0.098	0.076	0.007

Table 5
Case study 3, pose 2. Comparison between CMA-ES and SS results. Best minimum and mean values are highlighted in bold letters.

Case	Algorithm	Initialization	Evals (thousands)	Min.	Max.	Mean	St.Dev.
3, Pose 2	SS	No	30	**0.058**	0.069	0.063	0.003
3, Pose 2	SS	No	60	0.058	0.068	0.062	0.003
3, Pose 2	SS	No	100	0.058	0.068	0.062	0.003
3, Pose 2	SS	No	150	0.058	0.068	0.062	0.003
3, Pose 2	SS	No	300	0.058	0.068	0.062	0.003
3, Pose 2	SS	Yes	30	**0.058**	0.069	**0.059**	0.002
3, Pose 2	SS	Yes	60	0.058	0.064	0.059	0.001
3, Pose 2	SS	Yes	100	0.058	0.063	0.059	0.001
3, Pose 2	SS	Yes	150	0.058	0.063	0.059	0.001
3, Pose 2	SS	Yes	300	0.058	0.063	0.059	0.001
3, Pose 2	CMA-ES	No	30	**0.058**	0.331	0.256	0.101
3, Pose 2	CMA-ES	No	60	0.058	0.330	0.243	0.118
3, Pose 2	CMA-ES	No	100	0.058	0.318	0.101	0.079
3, Pose 2	CMA-ES	No	150	0.058	0.302	0.105	0.067
3, Pose 2	CMA-ES	No	300	0.058	0.149	0.070	0.026
3, Pose 2	CMA-ES	Yes	30	0.161	0.331	0.290	0.053
3, Pose 2	CMA-ES	Yes	60	0.156	0.331	0.293	0.062
3, Pose 2	CMA-ES	Yes	100	0.141	0.328	0.214	0.062
3, Pose 2	CMA-ES	Yes	150	0.142	0.323	0.219	0.066
3, Pose 2	CMA-ES	Yes	300	0.141	0.299	0.177	0.038

Table 6
Case study 4. Comparison between CMA-ES and SS results. Best minimum and mean values are highlighted in bold letters.

Case	Algorithm	Initialization	Evals (thousands)	Min.	Max.	Mean	St.Dev.
4	SS	No	30	**0.010**	0.043	0.019	0.008
4	SS	No	60	0.010	0.042	0.019	0.008
4	SS	No	100	0.010	0.042	0.019	0.008
4	SS	No	150	0.010	0.042	0.019	0.008
4	SS	No	300	0.010	0.042	0.019	0.008
4	SS	Yes	30	**0.010**	0.031	0.017	0.006
4	SS	Yes	60	0.010	0.029	0.017	0.006
4	SS	Yes	100	0.010	0.029	0.017	0.005
4	SS	Yes	150	0.010	0.029	0.017	0.005
4	SS	Yes	300	0.010	0.029	**0.016**	0.005
4	CMA-ES	No	30	0.063	0.284	0.261	0.051
4	CMA-ES	No	60	0.032	0.285	0.233	0.081
4	CMA-ES	No	100	0.029	0.275	0.105	0.087
4	CMA-ES	No	150	0.029	0.271	0.102	0.083
4	CMA-ES	No	300	0.029	0.251	0.069	0.055
4	CMA-ES	Yes	30	0.264	0.287	0.283	0.004
4	CMA-ES	Yes	60	0.265	0.287	0.283	0.005
4	CMA-ES	Yes	100	0.142	0.284	0.244	0.045
4	CMA-ES	Yes	150	0.139	0.283	0.231	0.044
4	CMA-ES	Yes	300	0.137	0.280	0.204	0.045

strategy has no influence (neither positive nor negative) over the quality of the best minimum result.

Nevertheless, the fact that the initialization allows the algorithm to become more robust can be easily checked in view of the mean and standard deviation values of the thirty runs performed collected in the six result tables. Notice that, the SS variant with initialization outperforms the variant not considering it in terms of mean results in all the problem instances considered. This performance advantage is also supported by the fact that it also achieves lower standard deviation values in all the cases but one (case study 1-pose 1, see Table 1). Nevertheless, we should note that only standard deviation loss is justified by an important reduction in the mean value.

Furthermore, the SS variant considering the initialization strategy has also shown to converge more quickly than its counterpart which does not make use of this component. We should highlight that the best mean value achieved for the latter SS variant after 300000 evaluations is always outperformed by the initialization-based SS taking a significantly lower number (and thus a shorter run time). This value is reduced to 100000 evaluations in two instances (case 1-pose 1, and case 3-pose 1), 60000 evaluations in two instances (case 1-pose 2, and case 2), and even to 30000 evaluations in the other two instances (case 3-pose 2, and case 4).

In view of these results, we can assert that the inclusion of initialization strategy performing a restriction on the rotation angles in the SS method implies a more robust behavior and a faster convergence.

4.3. Comparison with respect to the state-of-the-art results

In this second experimental study we focus on comparing the performance of the proposed SS algorithm with respect to that achieved by CMA-ES, which has shown as the best existing technique to solve the problem up to now (Ibáñez et al., 2009).

Fig. 10. Best skull-face overlay results for all the cases but case 4 (we are not able to publish it due to legal reasons). From left to right, overlay results over case 1-poses 1 and 2, and case 2 are depicted in the first row. Case 3-poses 1 and 2 overlay results are depicted in the second row. For all the cases, the first image corresponds to the CMA-ES result and the second to SS.

For this aim, we take into account the best configuration for CMA-ES and for SS. As it was demonstrated in Section 4.2, SS works better when the initialization strategy based on the rotation angles restriction is considered. Hance, in order to develop a fair comparison, we have incorporated that novel component to the CMA-ES-based skull-face overlay method proposed in Ibáñez et al. (2009). We have thus studied the behavior of CMA-ES algorithm with and without this initialization. Nevertheless, on the contrary to the SS case, this mechanism to reduce the search space does not manage to improve CMA-ES results, as can be seen in the two bottom blocks of Tables 1–6. Indeed, the algorithm's performance gets worse once we included the delimitation of the rotation angles. It seems that, although the advanced initialization induces an appropiate intensification-diversification trade-off within the SS design, that is not the case for CMA-ES which shows a less flexible structure.

Tables 1–6 show CMA-ES and SS results for the six cases of study. Due to the reasons cited in the paragraph before, we directly compare CMA-ES without initialization against SS with initialization.

On one hand, the best minimum values achieved by both algorithms are exactly the same for five of the six cases considered. They are only significantly different in case 4, where SS clearly outperforms CMA-ES (0.010 vs. 0.029, see Table 3).

On the other hand, if we focus on the mean values of the thirty runs, SS improves CMA-ES results, for all the tested number of evaluations, in three cases: case 3-poses 1, 2 and case 4 (see Tables 4–6). In the other three cases (case 1-poses 1, 2; and case 2) SS improves all CMA-ES results excepting for the case of 300000 evaluations. This results lead us to assert that SS converge more quickly than CMA-ES, despite the fact that when the number of evaluations is high (from 300000 evaluations), there are some cases where CMA-ES finally achieves a slightly better mean accuracy than SS.

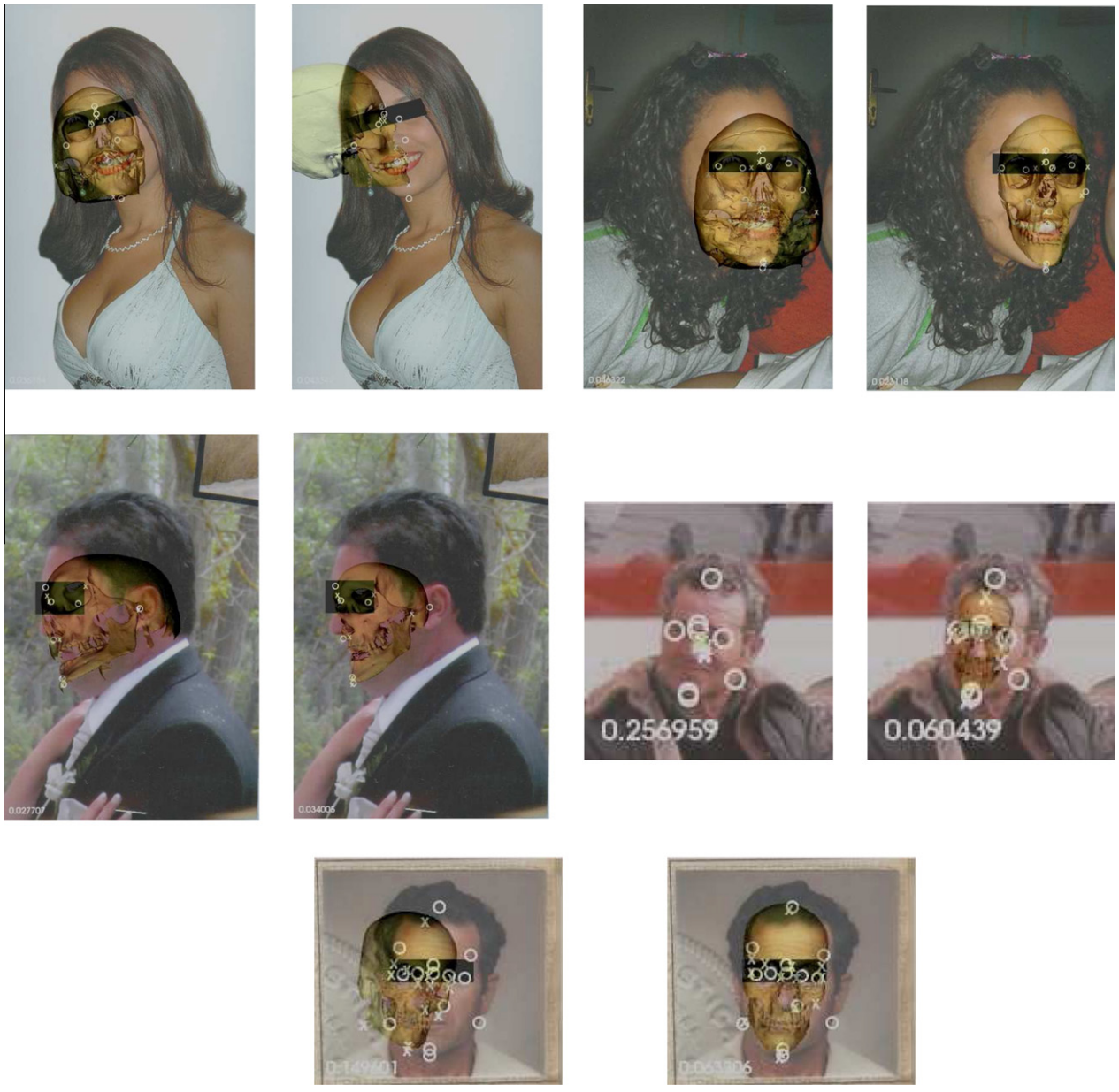

Fig. 11. Worst skull-face overlay results for all the cases but case 4 (we are not able to publish it due to legal reasons). From left to right, overlay results over case 1-poses 1 and 2, and case 2 are depicted in the first row. Case 3-poses 1 and 2 overlay results are depicted in the second row. For all the cases, the first image corresponds to the CMA-ES result and the second to SS.

Besides, we should notice the low standard deviation values obtained by SS, which are an additional proof of its robustness.

Finally, to allow for a visual inspection of the obtained overlays, Figs. 10 and 11 graphically represent best and worst skull-face overlay results obtained by the two algorithms in the thirty runs performed. These overlays correspond to the best configuration of CMA-ES and SS, after 300000 evaluations. In all the cases, the best overlays are almost the same. In contrast, the worst overlays obtained by SS are usually better than those provided by CMA-ES. The CMA-ES result is only better for case 1-pose 1. On the contrary, the SS results are slightly better in SS for case 1-pose 2 and case 3-pose 1, as well as much better for case 3-pose 2. In the remainder instance (case 2), both results could be considered as showing a similar low quality.

5. Concluding remarks and future works

In this paper, we have introduced the use of a novel metaheuristic framework, SS, as a new 3D-2D IR optimizer for the skull-face overlay task in forensic identification by craniofacial superimposition. Having in mind the interesting properties and the recent successful outcomes achieved by the former technique in other global optimization problems (Laguna & Martí, 2003), our starting point was focused on the suitable design of the SS components and the way they were assembled, in order to achieve faster and more robust solutions to the skull-face overlay problem.

We have proposed a method to properly initialize the algorithm and to restrict the parameter ranges using problem-specific information (domain knowledge). That "intelligent" initialization is based on the orientation of the skull to a frontal pose and the corresponding limitation of the rotation angles, which results in a significant reduction of the solution space, thus easing the problem solving.

We have presented and discussed skull-face overlay results obtained on six real-world identification cases. A sound experimental study to compare the robustness and convergence speed regarding the use of the proposed initialization has been performed. We have demonstrated the benefits (faster convergence and higher robustness) of including this advanced strategy in the proposed SS algorithm. Besides, we have shown how it does not properly cooperate with the existing CMA-ES design to solve the problem. The main experimentation dealt with a comparison between the proposed SS and our previous CMA-ES-based skull-face overlay procedure. Despite both algorithms have a really good behavior, achieving similar minima, our new proposal has been shown to converge faster than CMA-ES and to behave more robustly in view of the mean values obtained in the thirty runs developed.

These are really important issues in a real-world application. Regarding robustness we have to ensure accurate skull-face overlay results considering just a single run. Regarding velocity of convergence, a fast approach will be desirable in future developments as well. Indeed, considering different sources of uncertainty (see Ibáñez, Cordón, Damas, & Santamaría, 2009) will lead to more complex fitness function definitions that will demand more computing resources for their evaluation. Furthermore, a fast and robust approach allows a high number of reliable skull-face overlays in a short period of time. Thus, this method would be useful for the identification in image data bases of missing people.

For future work, we should consider that we are dealing with real-world craniofacial superimposition cases, where the thickness of the soft tissue, as well as the uncertainty of localizing landmarks, influence the final results of our automatic metaheuristic approach. Due to this reason, adding fuzzy logic to the process, a quite common action in environments where there is any source of inherent uncertainty like medicine (Yardimci, 2009), seems to be a good approach for future developments. Indeed, we have started working in this line proposing a first approach to the location uncertainty problem (Ibáñez et al., 2009) and we are planning to tackle the matching uncertainty in the short future using fuzzy distance measures (Guha & Chakraborty, 2010) by means of both the CMA-ES and the SS-based approaches.

Moreover, we aim to consider a higher number of real cases of identification provided and solved by the Physical Anthropology lab at the University of Granada, as well as negative cases.

Acknowledgments

This work is supported by the Spanish Ministerio de Educación y Ciencia (Ref. TIN2009-07727) and by the Andalusian Dpt. of Innovación, Ciencia y Empresa (Ref. TIC-1619), both including EDRF fundings. We would like to acknowledge all the team of the Physical Anthropology lab at the University of Granada (headed by Dr. Botella and Dr. Alemán) for their support during the data acquisition and validation processes. Part of the experiments related to this work was supported by the computing resources at the Supercomputing Center of Galicia (CESGA), Spain.

References

Al-Amad, S., McCullough, M., Graham, J., Clement, J., & Hill, A. (2006). Craniofacial identification by computer-mediated superimposition. *Journal of Forensic Odontostomal, 24*, 47–52.

Auger, A., & Hansen, N., (2005). A restart CMA evolution strategy with increasing population size, In *Proceedings of the IEEE congress on evolutionary computation CEC 2005*, (pp. 1769–1776).

Aulsebrook, M. Y., Iscan, W. A., Slabbert, J. H., & Becker, P. (1995). Superimposition and reconstruction in forensic facial identification: A survey. *Forensic Science International, 75*(2-3), 101–120.

Bilge, Y., Kedici, P., Alakoc, Y., Ulkuer, K., & Ilkyaz, Y. (2003). The identification of a dismembered human body: A multidisciplinary approach. *Forensic Science International, 137*, 141–146.

Burns, K. (2007). *Forensic Anthropology Training Manual*. Prentice-Hall.

Cordón, O., Damas, S., Martí, R., & Santamaría, J. (2008). Scatter search for the 3D point matching problem in image registration. *INFORMS Journal on Computing* (1), 55–68.

Cordón, O., Damas, S., & Santamaría, J. (2006). Feature-based image registration by means of the CHC evolutionary algorithm. *Image and Vision Computing, 24*(5), 525–533.

Cordón, O., Damas, S., & Santamaría, J. (2007). A practical review on the applicability of different EAs to 3D feature-based registration, In S. Cagnoni, E. Lutton, G. Olague (Eds.), *genetic and evolutionary computation in image processing and computer vision*, EURASIP Book Series on SP& C, (pp. 241–263).

Damas, S., Cordón, O., Ibáñez, O., Santamaría, J., Aleman, I., Navarro, F., & Botella, M. (in press). Forensic identification by computer-aided craniofacial superimposition: a survey, ACM Computing Surveys. in press.

Eiben, A., & Smith, J. (2003). *Introduction to Evolutionary Computing*. Springer-Verlag.

Eshelman, L. J. (1993). Real-coded genetic algorithms and interval schemata. In L. D. Whitley (Ed.), *Foundations of Genetic Algorithms 2* (pp. 187–202). San Mateo: Morgan Kaufman.

Fenton, T. W., Heard, A. N., & Sauer, N. J. (2008). Skull-photo superimposition and border deaths: Identification through exclusion and the failure to exclude. *Journal of Forensic Sciences, 53*(1), 34–40.

Foley, J. D. (1995). *Computer Graphics: Principles and Practice*. Addison-Wesley.

Gagné, C., Beaulieu, J., Parizeau, M., & Thibault, S. (2008). Human-competitive lens system design with evolution strategies. *Applied Soft Computing, 8*, 1439–1452.

Ghosh, A., & Sinha, P. (2001). An economised craniofacial identification system. *Forensic Science International, 117*(1-2), 109–119.

Glover, F. (1977). Heuristic for integer programming using surrogate constraints. *Decision Sciences*, 156–166.

Glover, F., Laguna, M., & Martí, R. (2003). Scatter search. In A. Ghosh & S. Tsutsui (Eds.), *Theory and Applications of Evolutionary Computation: Recent Trends* (pp. 519–537). Springer-Verlag.

Gonzalez, R., & Woods, R. (2002). *Digital Image Processing* (2nd ed.). Upper Saddle River, New Jersey: Prentice Hall.

Guha, D., & Chakraborty, D. (2010). A new approach to fuzzy distance measure and similarity measure between two generalized fuzzy numbers. *Applied Soft Computing, 10*, 90–99.

Hansen, N., & Ostermeier, A. (1996). Adapting arbitrary normal mutation distributions in evolution strategies: The covariance matrix adaptation, In *Proceedings of the IEEE international conference on evolutionary computation*, Piscataway, New Jersey, (pp. 312–317).

Hansen, N., & Ostermeier, A. (2001). Completely derandomized self-adaptation in evolution strategies. *Evolutionary Computation, 9*(2), 159–195.

Herrera, F., Lozano, M., & Molina, D. (2006). Continuous scatter search: An analysis of the integration of some combination methods and improvement strategies. *European Journal of Operational Research, 169*(2), 450–476.

Herrera, F., Lozano, M., & Verdegay, J. L. (1998). Tackling real-coded genetic algorithms: operators and tools for the behavioural analysis. *Artificial Intelligence Reviews, 12*(4), 265–319.

Ibáñez, O., Ballerini, L., Cordón, O., Damas, S., & Santamaría, J. (2009). An experimental study on the applicability of evolutionary algorithms to craniofacial superimposition in forensic identification. *Information Sciences, 179*, 3998–4028.

Ibáñez, O., Cordón, O., Damas, S., & Santamaría, J. (2009). A new approach to fuzzy location of cephalometric landmarks in craniofacial superimposition, In *international fuzzy systems association - european society for fuzzy logic and technologies (IFSA-EUSFLAT) world congress*, Lisbon, Portugal, (pp. 195–200).

Iscan, M. Y. (1993). Introduction to techniques for photographic comparison. In M. Y. Iscan & R. Helmer (Eds.), *Forensic Analysis of the Skull* (pp. 57–90). Wiley.

Kämpf, J. H., & Robinson, D. (2009). A hybrid CMA-ES and HDE optimisation algorithm with application to solar energy potential. *Applied Soft Computing, 9*, 738–745.

Krasnogor, N., & Smith, J. (2005). A tutorial for competent memetic algorithms: Model, taxonomy and design issues. *IEEE Transactions on Evolutionary Computation, 9*(5), 474–488.

Krogman, W. M., & Iscan, M. Y. (1986). *The human skeleton in forensic medicine* (2nd ed.). Springfield, IL: Charles C. Thomas.

Laguna, M., & Martí, R. (2003). *Scatter Search: Methodology and Implementations in C*. Kluwer Academic Publishers.

Lozano, M., Herrera, F., Krasnogor, N., & Molina, D. (2004). Real-coded memetic algorithms with crossover hill-climbing. *Evolutionary Computation, 12*(3), 273–302.

Lozano, M., Herrera, F., Krasnogor, N., & Molina, D. (2004). Real-coded memetic algorithms with crossover hill-climbing. *Evolutionary Computation, 12*(3), 273–302.

Michalewicz, Z. (1996). *Genetic Algorithms + Data Structures = Evolution Programs*. Springer-Verlag.

Nickerson, B. A., Fitzhorn, P. A., Koch, S. K., & Charney, M. (1991). A methodology for near-optimal computational superimposition of two-dimensional digital facial photographs and three-dimensional cranial surface meshes. *Journal of Forensic Sciences, 36*(2), 480–500.

Noman, N., & Iba, H. (1983). Enhancing differential evolution performance with local search for high dimensional function optimization. In *Genetic and evolutionary computation conference (GECCO'05)* (pp. 967–974). ACM.

Ross, A. H. (2004). Use of digital imaging in the identification of fragmentary human skeletal remains: A case from the Republic of Panama. *Forensic Science Communications, 6*(4).

Rouet, J. M., Jacq, J. J., & Roux, C. (2000). Genetic algorithms for a robust 3-D MR-CT registration. *IEEE Transactions on Information Technology in Biomedicine, 4*(2), 126–136.

Santamaría, J., Cordón, O., Damas, S., Alemán, I., & Botella, M. (2007). A scatter search-based technique for pair-wise 3D range image registration in forensic anthropology. *Soft Computing, 11*(9), 819–828.

Santamaría, J., Cordón, O., Damas, S., García-Torres, J. M., & Quirin, A. (2009). Performance evaluation of memetic approaches in 3D reconstruction of forensic objects. *Soft Computing, 13*(8-9), 883–904.

Silva, L., Bellon, O., & Boyer, K. (2005). *Robust Range Image Registration Using Genetic Algorithms and the Surface Interpenetration Measure*. World Scientific.

Sinha, P. (1998). A symmetry perceiving adaptive neural network and facial image recognition. *Forensic Science International, 98*(1-2), 67–89.

Stephan, C. N. (2009). Craniofacial identification: Techniques of facial approximation and craniofacial superimposition. In S. Blau & D. H. Ubelaker (Eds.), *Handbook of Forensic Anthropology and Archaeology* (pp. 304–321). California, USA: Left Coast Press.

Tvrdík, J. (2009). Adaptation in differential evolution: A numerical comparison. *Applied Soft Computing, 9*, 1149–1155.

Ubelaker, D. H. (2000). A history of Smithsonian-FBI collaboration in forensic anthropology, especially in regard to facial imagery. *Forensic Science Communications, 2*(4).

Yamany, S. M., Ahmed, M. N., & Farag, A. A. (1999). A new genetic-based technique for matching 3D curves and surfaces. *Pattern Recognition, 32*, 1817–1820.

Yardimci, A. (2009). Soft computing in medicine. *Applied Soft Computing, 9*, 1029–1043.

Zitova, B., & Flusser, J. (2003). Image registration methods: A survey. *Image and Vision Computing, 21*, 977–1000.